Intermediates and Products of the Hexachlorodisilane Cleavage of Group 14 Element Phosphanes and Amines − Molecular Structure of Di-*tert*-butyl(trichlorosilyl)phosphane in the Gas Phase Determined by Electron Diffraction and *ab Initio* Calculations

Wolf-W. du Mont,*[a] Lars Müller,[a] Reiner Martens,[a] Paul M. Papathomas,[b] Bruce A. Smart,[b] Heather E. Robertson,[b] and David W. H. Rankin*[b]

Keywords: Phosphanes / Disilanes / Disilanylamines / Germanes / Stannanes / Stannanes

Reactions of dialkyl(trimethylsilyl)phosphanes RR′PSiMe$_3$ (**1**: R, R′ = *t*Bu; **3**: R, R′ = *i*Pr; **5**: R = *i*Pr, R′ = *t*Bu) with Si_2Cl_6 provide stable trichlorosilylphosphanes RR′PSiCl$_3$ (**2**, **4**, **6**); the reactions of silyl- and stannylamines of *i*Pr$_2$NMMe$_3$ (M = Si: **11**; M = Sn: **12**) with Si_2Cl_6, however, provide the stable pentachlorodisilanylamine *i*Pr$_2$NSi$_2$Cl$_5$ (**13**). Heating of **1** with the technical mixture Me$_2$(Cl)SiSiCl$_2$Me/(MeCl$_2$Si)$_2$ yields the stable silylphosphane *t*Bu$_2$PSiMe$_2$Cl (**8**) and the disilanylphosphane *t*Bu$_2$PSi(Me)(Cl)Si(Me)Cl$_2$ (**9**). Methylation of **9** with MeLi gave *t*Bu$_2$PSi$_2$Me$_5$ **10**, which was isolated in a pure state. Reactions of *t*Bu(*i*Pr)PSiMe$_3$ (**5**) and of organometal phosphanes *t*Bu(*i*Pr)PMR$_3$ (**14**: M = Ge, R = Me; **17a–c**: M = Sn; R = Me, Et, *n*Bu) with Si_2Cl_6 were monitored by ^{31}P, ^{29}Si, and ^{119}Sn NMR. – In the first step of these reactions, new *t*Bu(*i*Pr)PSi$_2$Cl$_5$ (**7**) is formed. **7** is accompanied by increasing amounts of *t*Bu(*i*Pr)PSiCl$_3$ (**6**) and Me$_3$GeSiCl$_3$ (**15**)/(Me$_3$Ge)$_2$Si(SiCl$_3$)$_2$ (**16**) or traces of compounds R$_3$SnSiCl$_3$ (**19a–c**) that decompose providing (R$_3$Sn)$_2$Si(SiCl$_3$)$_2$ (**18a–c**) and *n*Bu$_3$SnSi(SiCl$_3$)$_3$ (**20c**). Subsequently, compounds **19a–c** decompose providing increasing amounts of **18a–c**. Stannylphosphane **17b** is also cleaved by SiCl$_4$ leading to **6** with liberation of Et$_3$SnCl, whereas **17b** *is formed* from the reaction of **5** with Et$_3$SnCl under liberation of Me$_3$SiCl. The suggestion of an extra stabilisation of P–Si bonds of trichlorosilylphosphanes was subjected to direct evidence through the structure determination of the trichlorosilylphosphane *t*Bu$_2$PSiCl$_3$ (**2**) in the gas phase by electron diffraction. This crowded molecule has a "normal" P–Si bond length of 225.0(12) pm; its C_1 symmetric conformation with both *t*Bu groups and the SiCl$_3$ group twisted about 17° from the perfectly staggered positions, and with each of the three groups tilted about 6° away from each other, allows to reduce steric strain.

Introduction

Trihalosilyl compounds are of importance as trifunctional precursors for the synthesis of highly functionalised silicon compounds. The cleavage of trimethylgermyl and -stannyl phosphanes with hexachlorodisilane was reported to furnish trichlorosilylphosphanes as well as trichlorosilyltrimethylgermane and trichlorosilyltrimethylstannane.[1] This novel reductive trichlorosilylation of Me$_3$Ge and Me$_3$Sn groups attached to phosphorus was thought to be due to nucleophilic attack of Me$_3$Ge and Me$_3$Sn groups by latent trichlorosilyl anions. Such anions are generated from one SiCl$_3$ group of Si_2Cl_6 when the other silicon atom is attacked by a phosphorus nucleophile leading to an adduct.[2] Because in situ-generated trichlorosilyl anions are also the key precursors in reactions of trichlorosilane/triethylamine mixtures with various organic halides leading to products of reductive *C*-trichlorosilylations,[3,4] we recently used the "Benkeser" type of reaction of chlorotrimethylstannane with the trichlorosilane/triethylamine reagent as an alternative route to trichlorosilyltrimethylstannane.[5] In the course of the extension of this type of reductive trichlorosilylation for the preparation of trihalosilyl derivatives of main group elements, we were surprised by the nature of the products from the trichlorosilane/triethylamine reagent with chlorotrimethylgermane[6] and dichlorodimethylgermane.[6,7] Contradictory data concerning liquid Me$_3$Ge−SiCl$_3$ and solid (Me$_3$Ge)$_2$Si(SiCl$_3$)$_2$[1,6] led us to study the "Benkeser" type of reaction of organotin and organogermanium halides with the trichlorosilane/triethylamine reagent in detail by heteronuclear NMR.[6,7]

$$Me_3GeCl + HSiCl_3 + NEt_3 \longrightarrow Me_3GeSiCl_3 + (Me_3Ge)_2Si(SiCl_3)_2 + HNEt_3Cl + SiCl_4\ (ref.^{[7]}) \quad (1)$$

$$4\ Me_3GeSiCl_3 \longrightarrow (Me_3Ge)_2Si(SiCl_3)_2 + SiCl_4 + 2\ Me_3GeCl \quad (2)$$

The observation of unexpected products of the constitution (Me$_3$M)$_2$Si(SiCl$_3$)$_2$ (M = Ge, Sn) from these reactions led us to reinvestigate also, by heteronuclear NMR-spectroscopy, the course of the hexachlorodisilane cleavage of P−Ge and P−Sn bonds which yields trichlorosilylphos-

[a] Institut für Anorganische und Analytische Chemie der Technischen Universität Braunschweig,
Hagenring 30, D−38106 Braunschweig, Germany
Fax: (internat.) +49 (0)531/ 391 5387
E mail: w.du-mont@tu-bs.de
[b] Department of Chemistry, The University of Edinburgh,
West Mains Road, Edinburgh, EH9 3JJ, U. K.
Fax: (internat.) +44 (0)131/ 650 6452
E mail: d.w.h.rankin@ed.ac.uk

  1434−1948/99/0808−1381 $ 17.50+.50/0

phanes accompanied by new trichlorosilyl compounds containing Si−Ge and Si−Sn bonds.[1] These reactions are expected to be related to the known cleavage of trimethylsilylphosphanes tBu$_2$PSiMe$_3$ (**1**) and tBuP(SiMe$_3$)$_2$ with hexachlorodisilane, which allowed the isolation of the related trichlorosilylphosphanes tBu$_2$PSiCl$_3$ (**2**) and tBuP(SiMe$_3$)(SiCl$_3$) in high yields.[8] As "model" phosphanes we chose silyl-, germyl-, and stannylphosphane derivatives containing the tBu(iPr)P group, which are moderately bulky and fairly accessible from the corresponding chlorophosphane on the HSiCl$_3$/NEt$_3$ pathway[5] followed by methylation and transmetalation reactions.[9]

Reactions of Hexachlorodisilane with Silyl-, Germyl-, and Stannylphosphanes Followed by NMR Spectroscopy

1. Reactions of Chlorodisilanes with Silylphosphanes

The reaction of Si$_2$Cl$_6$ with tBu$_2$PSiMe$_3$ (**1**) was reported to provide trichlorosilylphosphane tBu$_2$PSiCl$_3$ (**2**) in high yield under mild conditions.[8] Similarly, iPr$_2$PSiMe$_3$ (**3**) was easily cleaved to give iPr$_2$PSiCl$_3$ (**4**) in fair yield. After distillation of **2** and **4**, the residues contained orange oils that are expected to contain yet undefined polysilanes, possibly with a certain degree of SiPR$_2$ functions. Addition of Si$_2$Cl$_6$ to tBu(iPr)PSiMe$_3$ (**5**) at 0°C provided a red-brown solution, which turned brown on warming to room temperature. ^{31}P-NMR spectra showed that 5 min after mixing the compounds about 75% **5** was accompanied by about 8% of tBu(iPr)PSiCl$_3$ (**6**), 8% of tBu(iPr)PSi$_2$Cl$_5$ (**7**), and about 3−4% each of two other new phosphorus compounds. After 80 min compound **7** appeared as the main product. After 13 h, **5** was completely consumed and **6** became the main product (about 55%), accompanied by **7** (about 40%) and two other phosphanes. After 10 d at room temp. more than 90% of **6** and less than 10% of other phosphanes were present in solution.

$$\underset{\mathbf{1,3}}{R_2PSiMe_3} + Si_2Cl_6 \longrightarrow \underset{\mathbf{2,4}}{R_2PSiCl_3} + Me_3SiCl + \textit{other products} \quad (3)$$

1, 2: R = tBu[1]
3, 4: R = iPr

$$\underset{\mathbf{5}}{(t\text{Bu})(i\text{Pr})PSiMe_3} + Si_2Cl_6 \longrightarrow \underset{\mathbf{6}}{(t\text{Bu})(i\text{Pr})PSiCl_3} + \underset{\mathbf{7}}{(t\text{Bu})(i\text{Pr})PSi_2Cl_5} + SiCl_4 + Me_3SiCl + \textit{other products} \quad (4)$$

$$\mathbf{1} + Me_2(Cl)SiSiCl_2Me + (MeCl_2Si)_2 \longrightarrow \underset{\mathbf{8}}{t\text{Bu}_2PSiMe_2Cl} + \underset{\mathbf{9}}{t\text{Bu}_2PSi(Me)(Cl)Si(Me)Cl_2} \quad (5)$$

The reaction of tBu$_2$PSiMe$_3$ (**1**) with an excess of the industrial disilane fraction Me$_2$(Cl)SiSiCl$_2$Me/(MeCl$_2$Si)$_2$ required heating for several hours. Distillation provided satisfactory yields of the silylphosphane tBu$_2$PSiMe$_2$Cl (**8**)[10] as first fraction and the new disilanylphosphane tBu$_2$PSi(Me)(Cl)Si(Me)Cl$_2$ **9** as second fraction. Both compounds are thermally stable at room temperature, but very sensitive to oxygen and moisture. The constitution of **9** was confirmed by ^{1}H-, ^{13}C-, ^{29}Si-, and ^{31}P-NMR spectra. Disilanylphosphane **9** (about 50% yield) is obviously the product of a transsilylation of **1** with (MeCl$_2$Si)$_2$. The formation of **8** from **1** (24%) with Me$_2$(Cl)SiSiCl$_2$Me is more surprising. The formation of **8** by transsilylation of **1** with Me$_2$SiCl$_2$ is known to proceed significantly more slowly than the reaction of **1** with MeSiCl$_3$.[10] Adding **9** to an excess of methyllithium led to permethylation giving tBu$_2$PSi$_2$Me$_5$ (**10**), which was then isolated in a pure state.

2. Reactions of Si$_2$Cl$_6$ with iPr$_2$NMMe$_3$ (11: M = Si; 12: M = Sn)

Heating the mixture of Si$_2$Cl$_6$ and iPr$_2$NSiMe$_3$ (**11**) for 6 h at 60°C led to complete consumption of **11**. Distillation provided iPr$_2$NSi$_2$Cl$_5$ (**13**) in fair yield. The stannylamine **12** is more reactive: after mixing **12** and Si$_2$Cl$_6$ at 0°C and warming to room temperature, the formation of crude **13** and Me$_3$SnCl was quantitative.

$$\underset{\mathbf{11}: M = Si;\ \mathbf{12}: M = Sn}{i\text{Pr}_2NMMe_3} + Si_2Cl_6 \longrightarrow \underset{\mathbf{13}}{i\text{Pr}_2NSi_2Cl_5} + Me_3MCl \quad (6)$$

$$\underset{\mathbf{14}}{(t\text{Bu})(i\text{Pr})PGeMe_3} + Si_2Cl_6 \longrightarrow \mathbf{6} + \underset{\mathbf{15}}{\mathbf{7}} + Me_3GeSiCl_3 + \underset{\mathbf{16}}{(Me_3Ge)_2Si(SiCl_3)_2} + SiCl_4 + Me_3GeCl \quad (7)$$

3. Reaction of Si$_2$Cl$_6$ with tBu(iPr)PGeMe$_3$ (14)

Five minutes after mixing the starting materials, about 30% of **14** was consumed in favour of five new phosphorus compounds, among them **6** and **7**. After 3 h, 50% of **14** had been consumed, **6** was the main product and small amounts of **7** (among other P-containing compounds) were also present. A ^{29}Si-NMR spectrum confirmed the presence of Me$_3$GeSiCl$_3$ (**15**) (a rather broad signal, ^{29}Si = +17.7)[7] and (Me$_3$Ge)$_2$Si(SiCl$_3$)$_2$ (**16**) (two signals, at δ ^{29}Si = +16.8 and −84.9, the upfield one being less intense)[7] as well as SiCl$_4$. One peak of the ^{29}Si doublet, doublet pattern of **6** (from Si,P and Si,H couplings) shows "enhanced intensity", possibly due to accidental overlap with the singlet signal of another new germylsilane [δ ^{29}Si = +10.1; probably Me$_3$GeSi(SiCl$_3$)$_3$[9]]. This signal is quite intense in the earliest stage of the reaction. After several days, when **14** had been completely consumed and the crude yield of **6** was close to 90%, the ^{29}Si-NMR pattern of **6** exhibited the expected four lines of equal intensity. Evidence for the formation of Me$_3$GeCl was provided by ^{13}C-NMR spectra of the reaction mixture.

4. Reaction of Si$_2$Cl$_6$ with Stannylphosphanes tBu(iPr)PSnR$_3$ (17a−c: R = Me, Et, nBu)

***t*Bu(*i*Pr)PSnMe$_3$ (17a):** Twenty minutes after mixing the starting materials **17a** had been completely consumed. Silylphosphane **6** and the branched bis(stannyl)silane **18a** were the main products; small amounts of disilanylphosphane **7** (less than 10% of **6**, by ^{31}P-NMR), stannylsilane **19a** (about 25% of **18a**), and a further stannylsilane [δ ^{29}Si = +11.3

and −88; probably $Me_3SnSi(SiCl_3)_3$[9]] were also present. After 15 h, the crude yields (by NMR) of **6** and of **18a** were both more than 90%.

***t*Bu(*i*Pr)PSnEt$_3$ (17b):** After 5 min, **17b** had been consumed and large amounts of the disilanylphosphane **7** were present. Tin-NMR spectra showed the presence of large amounts of $Et_3SnSiCl_3$ (**19b**) accompanied by **18b**[7] and Et_3SnCl. From such a sample, mass spectrometric evidence for **19b** ($M^+ - Et$) was provided. Within one hour, however, trichlorosilylphosphane **6** and the branched bis(stannyl)silane **18b** became the main products at the expense of **7** and **19b**. Besides **18b**, the presence of a further branched silylstannane was indicated by ^{29}Si-NMR ($\delta\ ^{29}Si = +11.7$ and −88).

In an additional experiment, **17b** was mixed with $SiCl_4$ at room temperature. NMR spectra revealed that **17b** was consumed and that trichlorosilylphosphane **6** and Et_3SnCl were formed, accompanied by some *t*Bu(*i*Pr)PH.

$$\underset{\textbf{17a–c}}{(t\text{Bu})(i\text{Pr})\text{PSnR}_3} + \text{Si}_2\text{Cl}_6 \longrightarrow \textbf{6} + \textbf{7} + \underset{\textbf{19a–c}}{\text{R}_3\text{SnSiCl}_3} + \underset{\textbf{18a–c}}{(\text{R}_3\text{Sn})_2\text{Si}(\text{SiCl}_3)_2} \quad (8)$$

a: R = Me
b: R = Et
c: R = *n*Bu

$$+ \underset{\textbf{20a–c}}{\text{R}_3\text{SnSi}(\text{SiCl}_3)_3} + \text{SiCl}_4 + \text{R}_3\text{SnCl}$$

$$\underset{\textbf{17b}}{(t\text{Bu})(i\text{Pr})\text{PSnEt}_3} + \text{SiCl}_4 \longrightarrow \underset{\textbf{6}}{(t\text{Bu})(i\text{Pr})\text{PSiCl}_3} + \text{Et}_3\text{SnCl} \quad (9)$$

***t*Bu(*i*Pr)PSn(*n*Bu)$_3$ (17c):** as in the cases described above, consumption of the stannylphosphane **17c** was very fast. After 2 h, **7** and **19c**[7] were the main products and after 12 d, **6** and $n\text{Bu}_3\text{SnSi}(\text{SiCl}_3)_3$ (**20c**) were the predominant species. After an even longer reaction time (2 months), stannylsilane **19c** was completely decomposed and in addition to **20c**, the branched bis(stannyl)silane **18c** could also be detected by ^{29}Si- and ^{119}Sn-NMR.[7]

Discussion of the Reactions

1. Cleavage of Sn−N and Sn−P Bonds with Si_2Cl_6

Si_2Cl_6 cleaves stannylamines and stannylphosphanes quantitatively within a few minutes under mild conditions by transmetalation-like SnR_3/Si_2Cl_5 exchange reactions providing large amounts of the corresponding pentachlorodisilanylamines and -phosphanes and the trialkylchlorostannanes (Equation 6, Equation 10a). From such reactions, diisopropyl(pentachlorodisilanyl)amine **13** can be isolated in pure state; pentachlorodisilanylphosphane **7**, however, serves as a source of $SiCl_2$ or $SiCl_3^-$ moieties towards the trialkylchlorostannanes, leading by $Cl^-/SiCl_3^-$ exchange to trichlorosilylstannanes $R_3SnSiCl_3$ **19** (Equation 10b).

$$\textbf{17} + \text{Si}_2\text{Cl}_6 \xrightarrow{(10a)} \textbf{7} + \text{R}_3\text{SnCl} \xrightarrow{(10b)} \textbf{6} + \textbf{19} \quad (10)$$

$$4\ \textbf{19} \longrightarrow \textbf{18} + 2\ \text{R}_3\text{SnCl} + \text{SiCl}_4 \quad (11)$$

$$4\ \textbf{19} \longrightarrow \textbf{20} + 3\ \text{R}_3\text{SnCl} \quad (12)$$

$$\textbf{19} + 3\ \textbf{7} \longrightarrow \textbf{20} + 3\ \textbf{6} \quad (13)$$

These compounds can be detected by NMR in solution, but they are not persistent under the reaction conditions (presence of phosphorus nucleophiles). Their decomposition furnishes new branched stannylsilanes $(R_3Sn)_2Si(SiCl_3)_2$ **18** and $R_3SnSi(SiCl_3)_3$ **20** (Equations 11, 12). The previous assignments of NMR data of compounds **15** and **19a** made in ref.[1] have to be withdrawn (see the following section, Table 1). The isolated solids were not **15** and **19a**,[1] but **16** and **18a**.[7] The formation of compounds **20** from **19** (which is favoured by bulkier alkyl groups at tin) can be explained as being reaction steps analogous to those that occur in the course of the base-catalysed disproportionation of Si_2Cl_6, i.e. $Cl^-/SiCl_3^-$ exchange or $SiCl_2$ insertion at the most branched Si atom of an oligochlorosilane.[11–13] Disilanylphosphane **7** can also be a source of $SiCl_3^-$ or $SiCl_2$ (Equation 13). The predominant formation of bis(stannyl)silanes **18a**, **b** and the related germanium compound **16**[7] deserves further investigation; the formation of a second Si−Sn or Si−Ge bond leading from **15/19** to intermediates $(R_3M)_2SiCl_2$ (M = Ge, Sn) as precursors for **16/18** is apparently affected by bulkier alkyl groups at Ge or Sn.

2. Cleavage of Trimethylgermylphosphane 14 by Si_2Cl_6

This reaction proceeds much more slowly than the reaction of stannylphosphanes **17**. Disilanylphosphane **7** is already being consumed by its reaction with Me_3GeCl before its formation by the cleavage of **14** can be quantitative. Formation of trichlorosilylphosphane **6** is slower than in the stannylphosphane reactions, but finally it is also close to quantitative. Contribution of a *direct* $GeMe_3/SiCl_3$ exchange (that was previously proposed[1]) to the formation of $Me_3GeSiCl_3$ (**15**) and **6** cannot be ruled out. Even at an early phase of the reaction, approximately equal amounts of **15** and the branched bis(germyl)silane **16** are present in solution. Experiments with pure **15** show that the presence of Me_3GeCl (its decomposition product !) inhibits the base-catalysed decomposition.[7] The formation of deeply coloured precipitates on addition of Si_2Cl_6 to the phosphanes at 0°C deserves further attention. Phosphanes are known to catalyse the disproportionation,[14] they can coordinate with Si_2Cl_6,[2] and they can activate disilanes for radical reactions with $n\text{Bu}_3\text{SnH}$.[15]

3. Cleavage of Trimethylsilylphosphanes by Si_2Cl_6 and by the Disilane Fraction

Silylphosphane **5** reacts more slowly than the stannylphosphanes but faster than the germylphosphane **14** with Si_2Cl_6 (silylphosphane **5** requires more than 2 h, germylphosphane **14** about a day, and stannylphosphanes **17a-c** less than 20 min to be consumed completely). In the course of the decomposition of disilanylphosphane **7** in the presence of Me_3SiCl, the compound $Me_3SiSiCl_3$ was not detected by ^{29}Si NMR. This compound is known to disproportionate in the presence of N- or P-nucleophiles.[16] Silylphosphane **1** reacts with $(MeCl_2Si)_2$ by transsilylation yielding $t\text{Bu}_2\text{PSi(Me)(Cl)Si(Me)Cl}_2$ (**9**), a stable disilanylphosphane. $Me_2(Cl)SiSiCl_2Me$, however, suffered from Si−Si bond cleavage by **1** by attaching the chlorodimethylsilyl group to phosphorus, i.e. "the more electrophilic sily-

lene" MeSiCl (that allows better base-stabilisation) was lost when tBu$_2$PSiMe$_2$Cl (**8**) was formed. Whether **8** is in fact the *kinetic* product, i.e. whether the higher chlorinated silylphosphanes (like R$_2$PSiCl$_2$Me, R$_2$PSiCl$_3$) profit from extra stabilisation of their P−Si bonds compared with di- and trialkylsilylphosphanes, deserves further investigation.

Characterisation of New Germyl- and Stannylsilanes by NMR Spectroscopy

Assignments were supported by measurements on pure samples of **15** and **18a** from independent syntheses using the trichlorosilane/triethylamine route.[7]

In the series of compounds Me$_3$E−SiCl$_3$ (E = C, Si, Ge) the ^{29}Si resonances of the trichlorosilyl groups appear in the range 18 ± 1 ppm (Table 1). The ^{29}Si nuclei of the SiCl$_3$ groups of the branched compounds (Me$_3$E)$_2$Si(SiCl$_3$)$_2$ exhibit rather similar resonances. Our previous assignments of **15** and **19a**, however, were wrong[1]. Contributions from the electric field gradient (from the p-electron imbalance at Si) to σ_{para} will overcome inductive effects on δ^{29}Si (electronegativity range C >> Ge > Si, Sn). In the case of compounds Me$_3$ESiCl$_3$, however, the ^{13}C resonances of the methyl groups adjacent to C (δ = +24.4), Ge (δ = −2.8), and Sn (δ = −8.1) follow the inductive trend. Again, the related resonances of the branched compounds **16** and **18a** appear not far from those of **15** and **19a**.

The central silicon atoms of the branched bis(germyl)- and bis(stannyl)silanes (R$_3$E)$_2$Si(SiCl$_3$)$_2$ appear at rather low frequency, the tin compounds **18a−c** even lower frequency than the germanium derivative **16**. The ^{29}Si shift of the central atom of stannylsilane **20c** appears at significantly higher frequqency than that of the bis(stannyl)silane **18a**. The ^{119}Sn resonances of compounds **18a-c**, **19a-c**, and **20c** appear in a narrow range from δ = −45 to −70.[7]

Table 1. ^{13}C-, ^{29}Si-, and ^{119}Sn NMR shifts of trichlorosilyl derivatives of C, Si, Ge, and Sn and reference compounds

	δ^{13}C	δ^{29}Si	δ^{119}Sn
Me$_3$CSiCl$_3$	+24.37 [*C*H$_3$], +26.14 [*C*C$_3$]	+17.3	
Me$_3$SiSiCl$_3$[12]	*	+17.5 [*Si*Cl$_3$], −7.2 [*Si*Me$_3$]	
Me$_3$GeSiCl$_3$ **15**	−2.8	+17.8	
Me$_3$SnSiCl$_3$ **19a**	−8.6	*	−70[7]
Et$_3$SnSiCl$_3$ **19b**	*	*	−59
nBu$_3$SnSiCl$_3$ **19c**	*	*	−72
Si(SiCl$_3$)$_4$[17]		+3.5 [*Si*Cl$_3$], −80.0 [*Si*Si$_4$]	
(Me$_3$Ge)$_2$Si(SiCl$_3$)$_2$ **16**	+0.8	+17.2 [*Si*Cl$_3$], −84.2 [Ge$_2$*Si*Si$_2$]	
(Me$_3$Sn)$_2$Si(SiCl$_3$)$_2$ **18a**	−8.0	+19.6 [*Si*Cl$_3$], −106.4 [Sn$_2$*Si*Si$_2$]	−55.2
(Et$_3$Sn)$_2$Si(SiCl$_3$)$_2$ **18b**	+3.8 [Sn*C*] +12.1 [SnC*C*]	+21.0 [*Si*Cl$_3$], −108.2 [Sn$_2$*Si*Si$_2$]	−45.0
(nBu$_3$Sn)$_2$Si(SiCl$_3$)$_2$ **18c**	+12.2 [Sn*C*], +14.0 [SnC$_3$*C*], +27.8 [SnC$_2$*C*], +30.3 [SnC*C*]	+21.3 [*Si*Cl$_3$], −107.4 [Sn$_2$*Si*Si$_2$]	−52.7
nBu$_3$SnSi(SiCl$_3$)$_3$ **20c**		+12.0 [*Si*Cl$_3$,] −88.3 [Sn*Si*Si$_3$	−46.8

* Not available.

Table 2. ^{29}Si- and ^{31}P-NMR data of disilanylphosphanes and hexachlorodisilane adducts (δ in ppm, magitudes of J in Hz)

	δ ^{31}P	δ ^{29}*Si*(−P) |(^{1}J ^{29}Si, ^{31}P)|	δ ^{29}*Si*(−Si−P) |(^{2}J ^{29}Si, ^{31}P)|
tBu(iPr)PSiCl$_2$SiCl$_3$ **7**	8.3	13.2 (*125.5*)	−0.4 (*24.0*)
tBu$_2$PSiMeClSiMeCl$_2$ **9**	8.6	12.1 (*100.2*)	26.8 (*21.9*)
tBu$_2$PSiMe$_2$SiMe$_3$ **10**	5.6	−25.2 (*63.4*)	−14.9 (*12.1*)
iPr(iPr$_2$N)PSiCl$_2$SiCl$_3$[2]	42.7	8.9 (*132.0*)	1.1 (*16.6*)
iPr(iPr$_2$N)(Cl)PSiCl$_3$SiCl$_3$[2]	57.1	−69.6 (*160.7*)	9.8 (*24.8*)
tBu(Et$_2$N)PSiCl$_2$SiCl$_3$[2]	77.4	* (*134.2*)	* (*not resolved*)
tBu(Et$_2$N)(Cl)PSiCl$_3$SiCl$_3$[2]	98.0	* (*166.2*)	* (*24.3*)

Characterisation of New Disilanylphosphanes by NMR

Characteristic coupling patterns allowed safe assignments of the ^{31}P-NMR and ^{29}Si-NMR spectra of transient and persistent disilanylphosphanes (Table 2). Compared with organic subsituents or hydrogen, chlorine atoms at silicon lead to increased couplings ^1J and ^2J (^{31}P, ^{29}Si).[10,18] ^{29}Si-NMR shifts allow distinction between disilanylphosphanes (CN 4 at both Si) and phosphane-hexachlorodisilane adducts (one Si with CN 5 [low frequency], one Si with CN 4).[2]

Experimental and Calculated Structure of 2

Ab initio Calculations

Preliminary calculations on tBu$_2$PSiCl$_3$ were carried out at the 3-21G*/SCF level, assuming C_s symmetry. Vibrational-frequency calculations revealed the presence of a single imaginary frequency (74i cm^{-1}), indicating that the C_s structure represents a transition state connecting two equivalent C_1 minima. This structure can be regarded as

Table 3. Selected theoretical bond lengths, bond angles, and dihedral angles[a]

Parameter	3-21G*/ SCF	6-31G*/ SCF	6-31G*/ MP2
P−Si	225.0	227.0	224.9
Si−Cl(mean)	204.8	206.1	205.8
P(1)−C(6)	189.6	191.8	190.7
P(1)−C(19)	189.8	192.0	191.0
C−C(mean)	155.0	154.0	153.4
C−H(mean)	108.3	108.4	109.4
P(1)−Si(2)−Cl(3)	118.2	118.2	118.4
P(1)−Si(2)−Cl(4)	108.8	109.0	108.5
P(1)−Si(2)−Cl(5)	111.9	112.0	111.5
Si(2)−P(1)−C(6)	105.5	106.3	104.9
Si(2)−P(1)−C(19)	104.6	105.4	103.9
C(6)−P(1)−C(19)	111.4	111.8	111.0
P(1)−C(6)−C(7)	106.4	106.2	105.7
P(1)−C(19)−C(20)	108.5	108.2	107.6
C−C−H(mean)	110.7	111.2	110.8
Cl(5)−Si(2)−P(1)−C(19)	−164.7	−166.1	−164.8
C(20)−C(19)−P(1)−C(6)	−161.3	−162.4	−160.8
C(8)−C(6)−P(1)−Si(2)	−163.4	−164.0	−162.6

[a] All distances (r_a) in pm, all angles in°. See Figure 1 for atom numbering.

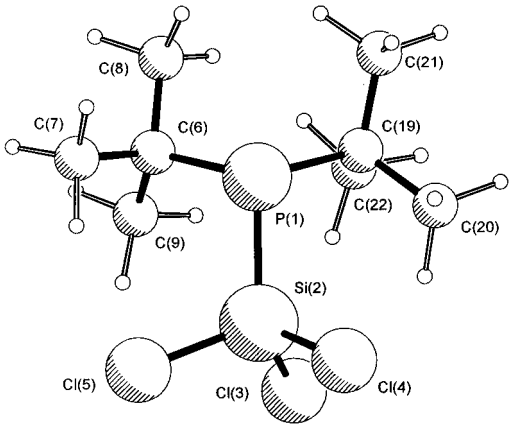

Figure 1. The molecular structure of tBu$_2$PSiCl$_3$ as determined by gas-phase electron diffraction

being derived from a fully staggered structure with *tert*-butyl and $SiCl_3$ groups twisted in the same sense by around 15−20°, increasing the minimum distance between H atoms on neighbouring *tert*-butyl groups from 195.4 pm (C_s) to 211.1 pm (C_1) and reducing the molecular energy by 16.8 kJ mol^{-1} at the 3-21G*/SCF level of theory. All subsequent calculations were carried out in C_1 symmetry. Selected geometric parameters are shown in Table 3 and the atom numbering is shown in Figure 1.

The computational facilities available to us restricted geometry optimisations to the 3-21G*/SCF, 6-31G*/SCF, and 6-31G*/MP2 levels, which should give an acceptably accurate geometry, since tBu$_2$PSiCl$_3$ is not expected to contain any significant multiple-bond character and there are few electronegative atoms.

With the 6-31G* basis set, raising the level of theory from SCF to MP2 produced little change (Table 3). Bond lengths were generally within ca. 1 pm; for example, the Si(2)−Cl(3) bond length is predicted to be 206.6 and 206.5 pm at the SCF and MP2 levels, respectively, and similarly the P(1)−C(19) bond length to be 192.0 and 191.0 pm at the same levels. Only the P−Si bond length changed appreciably, shortening from 227.0 pm to 224.9 pm. Bond angles generally varied by little more then 1°, although angles around the central phosphorus atom differed by up to 2°. At the SCF level the Si−P−C(6), Si−P−C(19), and C(6)−P−C(19) bond angles were predicted to be 106.3°, 105.4°, and 111.8° and to 104.9°, 103.9°, and 111.0° at the higher level.

Although the overall symmetry of tBu$_2$PSiCl$_3$ is predicted to be C_1, the $SiCl_3$ and two *tert*-butyl groups were all found to exhibit approximate local C_3 symmetry. At the 6-31G*/MP2 level, the calculated Si−Cl bond lengths lie in the range 205.4 to 206.5 pm, with internal Cl−Si−Cl angles ranging from 105.3° to 106.5°. Similarly, for the *tert*-butyl groups the C−C bond lengths are calculated to range from 153.0 to 153.7 pm, with internal P−C−C angles from 106.9° to 109.9°.

Molecular Model

The large number of geometric parameters needed to define the structure of tBu$_2$PSiCl$_3$ in C_1 symmetry made it necessary to introduce a number of assumptions into the GED refinement. At first the tBu and $SiCl_3$ groups had no symmetry and 9 parameters were used to define the C-(methyl) and Cl positions in each groups. The number of parameters was reduced only when (a) they were shown to be defined effectively entirely by restraints and (b) they were uncorrelated with the refining parameters. This procedure allows deviations from local symmetry to be fully explored rather than applying local symmetry without testing the validity of the assumptions. In this case the refined structures of *tert*-butyl and $SiCl_3$ groups showed insignificant variation from C_3 local symmetry. Therefore all further refinements were carried out assuming this symmetry. Moreover, within the levels of experimental uncertainty all six C−C bond lengths were also found to be indistinguishable and therefore were constrained to be equal. Since hydrogen

Table 4. Refined and calculated geometric parameters (distances in pm, angles in°) from the GED study[a]

No.	Parameter	GED(r_a)	6−31G*/MP2 (r_e)
a) independent parameters			
p_1	C−H	113.6(4)	109.4[b]
p_2	C−C	153.6(2)	153.4[b]
p_3	P−C (mean)	192.5(10)	190.9
p_4	P−C (diff)	−0.1(5)	−0.3
p_5	Si−Cl	204.7(3)	205.8[b]
p_6	P−Si	225.0(12)	224.9
p_7	C−C−H	109.2(9)	110.0[b]
p_8	P−C−C (mean)	109.2(4)	110.6
p_9	P−C−C (diff)	0.05(51)	−0.07
p_{10}	P−Si−Cl (mean)	112.9(2)	113.1
p_{11}	$SiCl_3$ torsion	194.1(15)	
p_{12}	$SiCl_3$ axial tilt	6.0(6)	
p_{13}	$SiCl_3$ equat. tilt	−0.5(19)	
p_{14}	Methyl twist	6.2(19)	
p_{15}	Methyl tilt	0.0(fixed)	
p_{16}	Butyl torsion (mean)	18.1(21)	
p_{17}	Butyl torsion (diff)	288.3(10)	
p_{18}	Butyl axial tilt (mean)	5.9(6)	
p_{19}	Butyl axial tilt (diff)	−1.2(14)	
p_{20}	Butyl equat. tilt (mean)	−0.7(4)	
p_{21}	Butyl equat. tilt (diff)	−4.0(7)	
p_{22}	Butyl dip (mean)	−31.5(8)	
p_{23}	Butyl dip (diff)	4.4(27)	
p_{24}	Butyl dihedral	105.4(7)	
b) dependent parameters			
p_{25}	C(6)−P−C(19)	110.6(13)	111.0
p_{26}	Si−P−C(6)	103.4(8)	104.9
p_{27}	Si−P−C(19)	102.8(6)	103.9
p_{28}	P−Si−Cl(3)	118.8(7)	118.4
p_{29}	P−Si−Cl(4)	108.9(16)	108.5
p_{30}	P−Si−Cl(5)	110.6(16)	111.5
p_{31}	P−C(6)−C(7)	104.9(10)	105.7
p_{32}	P−C(6)−C(8)	107.6(10)	108.5
p_{33}	P−C(6)−C(9)	114.9(10)	116.2
p_{34}	P−C(19)−C(20)	106.3(8)	107.6
p_{35}	P−C(19)−C(21)	105.3(8)	106.4
p_{36}	P−C(19)−C(22)	115.7(9)	116.8
p_{37}	Cl(5)−Si−P−C(19)	−163.4(16)	−164.8
p_{38}	C(20)−C(19)−P−C(6)	−156.5(23)	−160.8
p_{39}	C(8)−C(6)−P−Si	−161.8(21)	−162.6

[a] See text for atom numbering and parameter definitions. − [b] *ab initio* values quoted are mean values.

atom positions are poorly defined by the experimental data, all CH_3 groups were assumed to be identical and to have local C_{3v} symmetry.

In total 24 independent geometrical parameters were used to describe the structure of tBu$_2$PSiCl$_3$ in C_1 symmetry (Table 4). The bond length parameters are C−H, p_1, C−C, p_2, the mean and difference of P(1)−C(6) and P(1)−C(19), p_3 and p_4, Si−Cl, p_5, and P−Si, p_6. The bond angles are C−C−H, p_7, the average of the P−C−C bond angles, p_8, the difference between the averages of the P−C−C bond angles found in each of the *tert*-butyl groups, p_9, and the average P−Si−Cl angle, p_{10}.

The remaining parameters are best described with a coordinate system in which the P−Si bond defines the z axis, with P(1) at the origin and Si(2) in the positive z direction. The Cl atoms are arranged initially so that the z axis is an axis of local 3-fold symmetry, with Cl(3) lying in the xz plane in the positive x direction. By assuming a right-handed set of coordinate axes the y axis is also defined.

The $SiCl_3$ torsion angle is a rotation about the z axis, p_{11}, anticlockwise when viewed down the axis from Si to P. The $SiCl_3$ axial and equatorial tilts are anticlockwise rotations at Si(2) about the y axis, p_{12}, and the x axis, p_{13}, respectively. All subsequent torsion and tilt angle directions are anticlockwise when viewed down the rotation axis.

The *tert*-butyl groups were generated by initially placing a methyl group carbon at the origin [i.e. same position as P(1)] so that its three H atoms were arranged with local C_{3v} symmetry about the z axis and one H in the xz plane in the positive x direction. The methyl torsion, p_{14}, and tilt, p_{15}, are rotations about the z axis and x axis, respectively. The methyl group is then translated along the positive z axis by the average C−C bond length and the central carbon of the *tert*-butyl group is placed at the origin. The correct P−C−C bond angle is generated by rotating the methyl group about the y axis. The two remaining methyl groups are defined by replicating the first methyl group and then rotating about the z axis by 120° and −120°, respectively. The *tert*-butyl torsion angle is a rotation of the group about the z axis, while the axial and equatorial tilts are rotations about the y axis and x axis, respectively. Positive axial tilts move *tert*-butyl or $SiCl_3$ groups towards the phosphorus lone pair and equatorial tilts move these groups around the 3-fold belt. Parameters introduced here are the mean and difference of the butyl torsion angles, p_{16} and p_{17}, mean and difference of the butyl axial tilts, p_{18} and p_{19}, and the mean and difference of the butyl equatorial tilts, p_{20} and p_{21}. The *tert*-butyl groups are then translated along the positive z axis by their respective P−C bond lengths.

The three groups that were initially placed along the z axis are moved into their final positions by rotating both *tert*-butyl groups about the y axis by their respective "dip" angles to allow a nonplanar PC_2Si fragment, and then about the x axis by an equal amount in opposite directions to give the correct angles about phosphorus. This introduces three final parameters: the mean and difference of the butyl dip angles, p_{22} and p_{23}, and the *tert*-butyl rotation angle, p_{24}.

Electron Diffraction Refinement

The radial distribution curve for tBu$_2$PSiCl$_3$ (Figure 2) consists of five distinct peaks at distances of ca. 110, 155, 205, 280, and 340 pm together with shoulders and weaker peaks above 400 pm. The peaks at 110 and 155 pm correspond to C−H and C−C scattering, respectively, and the intense peak at 205 pm to scattering from Si−Cl bonds, broadened by contributions associated with the P−Si and P−C bonds. The peak at 280 pm consists mainly of scattering from P···C non-bonded pairs, while the intense broad peak at 340 pm is attributed to scattering from a number of nonbonded atom pairs, with major contributions from Cl···Cl and P···Cl pairs.

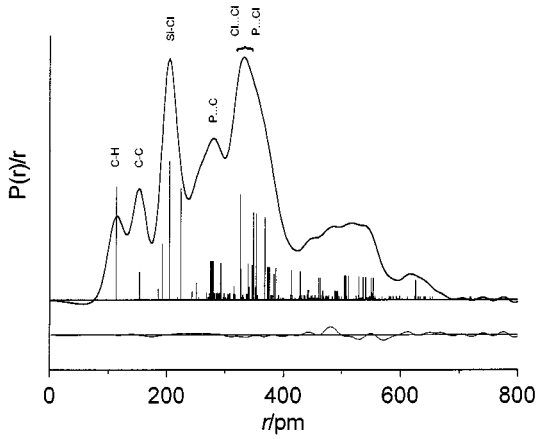

Figure 2. Experimental and difference (experimental − theoretical) radial distribution curves, $P(r)/r$, for tBu$_2$PSiCl$_3$. Before Fourier inversion the data were multiplied by $s\cdot\exp(-0.00002s^2)/(Z_{Si} - f_{Si})(Z_{Cl} - f_{Cl})$.

The starting parameters for the r_a structure refinement were taken from the theoretical geometry optimised at the 6-31G*/MP2 level. The program ASYM40[19] was used to convert the theoretical (6-31G*/SCF) Cartesian force field to one described by symmetry coordinates and this was scaled to obtain root-mean-square amplitudes of vibration (u). Scaling factors were chosen to be 0.90, 0.85, and 0.80 for bond stretches, angle bends and torsions, respectively. The presence of a large number of low-frequency vibrational modes led to overestimated predictions of the perpendicular amplitudes of vibration (k). Since these values were considered to be unreliable, corrections for shrinkage effects were not included.

Since the molecular structure contained a large number of similar interatomic distances, the SARACEN method[20] was employed in the GED refinements. Twelve geometrical and twelve vibrational amplitude restraints were used (Table 5). Values for geometrical restraints were taken to be those predicted at the 6-31G*/MP2 level, while amplitude restraints were based upon the force-field calculations at the 6-31G*/SCF level. Uncertainties were 0.5 pm for bond length differences, 1° for bond angles and 0.5° for bond angle differences. Torsion angles were assigned uncertainties of 2°, and 1° for differences. Uncertainties of 10% were assigned to vibrational amplitude restraints. The methyl tilt

Table 5. Flexible restraints

Number	Description	Parameter definition	Calculated value (Uncertainty)	Refined value
Geometrical restraints:				
1	P−C bond length difference	p_4	−0.2(5)	−0.14
2	Mean C−C−H angle	p_7	109.5(10)	109.2
3	P−C−C angle difference	p_9	−0.07(50)	0.05
4	Methyl torsion angle	p_{11}	4.0(20)	6.2
5	$SiCl_3$ torsion angle	p_{13}	194.0(20)	194.1
6	Butyl torsion angle difference	p_{17}	288.0(10)	288.3
7	C(6)−P−C(19) angle	p_{25}	111.0(10)	110.6
8	[Si−P−C(6)] − [Si−P−C(19)]	$p_{26} - p_{27}$	1.03(50)	0.6
9	P−C(6)−C(7) angle	p_{31}	105.7(10)	104.9
10	[P−C(6)−C(8)] − [P−C(6)−C(9)]	$p_{32} - p_{33}$	−7.7(10)	−7.3
11	[P−C(19)−C(20)] − [P−C(19)−C(21)]	$p_{34} - p_{35}$	1.1(5)	1.0
12	P−C(19)−C(22) angle	p_{36}	116.9(10)	115.7
Vibrational Restraints:				
13	P(1)−Si(2)	u_1	5.9(6)	5.5
14	P(1)···C(6)	u_2	5.8(6)	5.6
15	P(1)···Cl(3)	u_7	10.1(10)	8.9
16	Si(2)···C(6)	u_{16}	9.2(10)	9.3
17	Si(2)···C(7)	u_{18}	12.5(10)	12.4
18	Si(2)···C(8)	u_{19}	9.5(10)	10.7
19	Si(2)···C(9)	u_{20}	15.3(10)	15.4
20	Cl(3)···C(6)	u_{25}	18.9(20)	19.8
21	Cl(3)···C(7)	u_{27}	20.5(20)	22.7
22	Cl(3)···C(8)	u_{28}	20.0(20)	21.5
23	Cl(3)···C(9)	u_{29}	27.8(30)	24.8
24	Cl(4)···C(8)	u_{36}	12.3(10)	12.6

parameter, p_{12}, which helped define the position of the hydrogen atoms, was fixed, since little information is contained in the experimental data because of the poor scattering ability of hydrogen.

The use of flexible restraints allowed the refinement of 41 independent parameters, comprising 23 geometrical parameters and 18 amplitudes of vibration.

In the final refinement the R factors R_G and R_D were 0.091 and 0.077 respectively. Experimental and calculated radial distribution curves are shown in Figure 2, while Figure 3 displays the experimental and calculated molecular scattering intensity curves. Final refined parameters are listed in Table 4, selected interatomic distances and the corresponding amplitudes of vibration in Table 6 and the least-squares correlation matrix in Table 7.

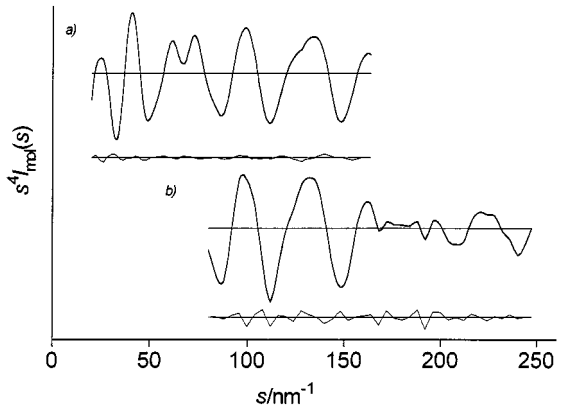

Figure 3. Experimental and final weighted difference (experimental − theoretical) molecular scattering intensities for tBu$_2$PSiCl$_3$. Camera distances were *(a)* 259 mm and *(b)* 95 mm

Discussion

The SARACEN method[20] has allowed the refinement of all significant structural parameters for tBu$_2$PSiCl$_3$. The highest possible molecular symmetry is C_s, but the perfectly staggered arrangement of all *tert*-butyl and $SiCl_3$ groups leads to parallel 1:3 interactions between two methyl groups or between a methyl group and a chlorine atom. The steric interactions of Y(MX$_3$)$_3$ groups are typically minimised by twisting the three groups by 15−20°, and this is what happens in this case, reducing the symmetry to C_1.

Overall, good agreement between theory and experiment was found; theoretical bond-length, bond-angle, and dihedral-angle predictions were in general found to be within one or two standard deviations of the experimental value. The introduction of electron correlation at the MP2 level is seen to be important in obtaining an accurate prediction of the P−Si distance; the 6-31G*/MP2 value at 224.9 pm is essentially identical to the experimental value of 225.0(12) pm, whilst the 6-31G*/SCF uncorrelated computation overestimates the distance at 227.0 pm. The P−Si bond length is also effectively identical to those found by GED in other compounds such as silylphosphane[21] [224.9(3) pm], silylmethylphosphane[21] [224.8(3) pm] and silyldimethylphosphane[21] [224.5(3) pm]. In H_2P-SiF_3, P−Si has been found[22] to be 220.7(3) pm, consistent with the fact that fluorine substituents at silicon result in a significant shortening of the P−Si bond length relative to that of H-substituted compounds. Substitution of the less electronegative chlorine for the silyl hydrogens does not seem to have a significant effect.[2]

Table 6. Selected interatomic distances (r_a) and root-mean-square amplitudes of vibration for tBu$_2$PSiCl$_3$ from the GED study[a]

Number	Atom pair	r_a/pm	u/pm
1	P−Si	225.0(12)	6.9(5)
2	P−C(6)	192.4(10)	5.6(1)
3	P−C(19)	192.5(10)	5.6(tied to u_2)
4	Si−Cl	204.7(3)	4.2(5)
5	C−C	153.6(2)	4.2(6)
6	C−H	113.6(2)	6.9(5)
7	P···Cl(3)	370.1(20)	8.9(9)
8	P···Cl(4)	350.0(40)	9.8(tied to u_7)
9	P···Cl(5)	353.5(33)	9.8(tied to u_7)
10	P···C(7)	275.4(18)	9.8(10)
11	P···C(8)	280.1(16)	10.1(tied to u_{10})
12	P···C(9)	292.4(16)	9.3(tied to u_{10})
13	P···C(20)	277.9(13)	10.0(tied to u_{10})
14	P···C(21)	276.1(13)	9.7(tied to u_{10})
15	P···C(22)	293.8(18)	9.4(tied to u_{10})
16	Si···C(6)	328.2(40)	9.2(10)
17	Si···C(19)	329.9(38)	9.0(tied to u_{16})
18	Si···C(7)	375.4(62)	12.4(10)
19	Si···C(8)	463.6(29)	10.7(9)
20	Si···C(9)	340.2(53)	15.4(10)
21	Si···C(20)	327.1(72)	13.4(tied to u_{20})
22	Si···C(21)	460.8(34)	10.9(tied to u_{19})
23	Si···C(22)	384.0(36)	13.5(tied to u_{18})
24	Cl(3)···Cl(4)	326.7(6)	10.1(6)
25	Cl(3)···C(6)	429.9(68)	19.8(19)
26	Cl(3)···C(19)	388.0(70)	15.5(tied to u_{28})
27	Cl(3)···C(7)	511.9(88)	22.7(19)
28	Cl(3)···C(8)	551.2(62)	21.5(13)
29	Cl(3)···C(9)	369.0(106)	24.8(27)
30	Cl(3)···C(20)	375.1(124)	23.8(tied to u_{28})
31	Cl(3)···C(21)	541.2(66)	18.5(tied to u_{27})
32	Cl(3)···C(6)	369.1(68)	19.3(tied to u_{28})
33	Cl(4)···C(6)	505.2(42)	12.4(tied to u_{26})
34	Cl(4)···C(19)	415.3(64)	15.3(tied to u_{24})
35	Cl(4)···C(7)	536.4(61)	19.4(tied to u_{27})
36	Cl(4)···C(8)	625.7(38)	12.6(9)
37	Cl(4)···C(9)	541.6(50)	15.8(tied to u_{27})
38	Cl(4)···C(20)	340.0(93)	16.5(tied to u_{28})
39	Cl(4)···C(21)	529.7(80)	18.9(tied to u_{27})
40	Cl(4)···C(22)	507.0(59)	20.9(tied to u_{26})
41	Cl(5)···C(6)	375.2(50)	13.3(tied to u_{28})
42	Cl(5)···C(19)	506.3(25)	11.5(tied to u_{26})
43	Cl(5)···C(7)	345.1(90)	15.0(tied to u_{28})
44	Cl(5)···C(8)	528.1(50)	15.9(tied to u_{27})
45	Cl(5)···C(9)	372.3(66)	21.6(tied to u_{28})
46	Cl(5)···C(20)	528.1(62)	14.1(tied to u_{27})
47	Cl(5)···C(21)	625.0(29)	12.2(tied to u_{35})
48	Cl(5)···C(22)	553.3(29)	17.4(tied to u_{27})
49	C(7)···C(8)	251.3(7)	4.5(9)

[a] See Figure 1 for atom numbering; all other distances were included in the refinement, but are not listed here.

All P−Si−Cl angle predictions were within one standard deviation of the experimentally determined values, and angles about the central phosphorus within two standard deviations. The angles about the central phosphorus [C−P−C 110.6(3)° and Si−P−C 103.6(3)°] are considerably larger than for the corresponding angles in silyldimethylphosphane[20] [C−P−C 100.8(12)° and Si−P−C 99.0(5)°], but can be attributed to the strong electron withdrawing character of the $SiCl_3$ group and to steric interactions between the *tert*-butyl groups. Axial tilts are all close to 6°, implying that $SiCl_3$ and *tert*-butyl groups are all tilted away from each other and towards the phosphorus lone pair. The equatorial tilts of the *tert*-butyl groups are smaller (ca. 2°) and towards one another. This implies that the residual steric interactions between two *tert*-butyl groups (after widening of the angle) are less than those between *tert*-butyl and $SiCl_3$ groups

Table 7. Least-squares correlation matrix (×100) for tBu$_2$PSiCl$_3$[a]

	p_3	p_5	p_6	p_{11}	p_{16}	p_{18}	u_1	u_5	u_6	u_{24}	k_1
p_6		74									
p_8	−64						−53				
p_{12}				−58							
p_{13}					−50						
p_{20}					−53						
p_{24}		−54	−62								
u_2		−53									
u_4							60				
u_{10}						68					
u_{49}			−50								
k_1	−50		50					73	52	57	
k_2			59					64	51	58	83

[a] Only elements with absolute values ≥ 50% are shown; k_1 and k_2 are scale factors.

Experimental Section

General: ^{1}H-, ^{13}C-, ^{29}Si-, and ^{31}P-NMR spectra: Bruker AC-200 spectrometer (200 MHz for ^{1}H, 50.3 MHz for ^{13}C, 81 MHz for ^{31}P, 39.8 MHz for ^{29}Si); solvent [D$_6$]benzene; shifts are given relative to TMS (^{1}H, ^{13}C, ^{29}Si) and 85% H_3PO_4 (^{31}P). − MS: Finnigan Mat 8430. − Elemental analyses: Carlo Erba analytical gas chromatograph. − All experiments were carried out under deoxygenated dry nitrogen as inert gas; solvents were dried according to standard procedures.

Ab initio Calculations: All calculations were performed on Dec Alpha 1000 4/200 and 8400 3/500 computers using the GAUSSIAN94 program.[23] Geometry optimisations were performed using the standard 3-21G*[24−26] and 6-31G*[27−29] basis sets at the SCF level and at the correlated MP2 level with the 6-31G* basis. Vibrational frequencies were calculated from analytic second derivatives at the 3-21G*/SCF and 6-31G*/SCF levels to determine the nature of stationary points and to provide estimates of amplitudes of vibration (u) for use in the GED refinements.

Electron Diffraction Measurements: Electron scattering intensities were recorded on Kodak Electron Image plates with the Edinburgh gas-diffraction apparatus operating at ca. 44.5 kV (electron wavelength ca. 5.7 pm).[30] Nozzle-to-plate distances for the metal inlet nozzle were 94.7 and 259.2 mm yielding data in the range s 20−360 nm^{-1}; four and three plates were exposed at the short and long distances, respectively. The sample and nozzle temperatures were maintained at ca. 423 and 448 K respectively during the exposure periods.

The scattering pattern of benzene was also recorded for the purpose of calibration; this was analysed in exactly the same way as for tBu$_2$PSiCl$_3$ so as to minimise systematic errors in the wavelengths and camera distances. Nozzle-to-plate distances, weighting functions used to set up the off diagonal weight matrix, correlation parameters, final scale factors and electron wavelengths for the measurements are collected in Table 8.

The electron scattering patterns were converted into digital form with a computer-controlled Joyce Loebl MDM6 microdensitometer and a scanning program described elsewhere.[31] The programs used for data reduction[31] and least squares refinement[32] have been

Table 8. Nozzle-to-plate distances [mm], weighting functions [nm^{-1}], correlation parameters and electron wavelengths [pm] used in the electron diffraction study

Nozzle-to-plate distance[a]	Δs	s_{min}	sw_1	sw_2	s_{max}	Correlation Parameter	Scale Factor[b]	Electron Wavelength
94.67	4	80	100	210	248	0.391	0.432(19)	5.653
259.17	2	20	40	140	164	0.411	0.638(24)	5.708

[a] Determined by reference to the scattering pattern of benzene. – [b] Values in parentheses are estimated standard deviations.

Table 9. ^{31}P-NMR data of *t*Bu(*i*Pr)PSiMe$_3$ (**5**), *t*Bu(*i*Pr)PSi$_2$Cl$_5$ (**7**), and *t*Bu(*i*Pr)PSiCl$_3$ (**6**)

time	**5**		**7**		**6**		other signals	
	[ppm]	relative intensity	[ppm]	relative intensity	[ppm]	relative intensity	[ppm]	relative intensity
5 min	−17.4	100	7.9	9	6.4	10	9.6	4
							10.8	5
30 min	−17.4	100	8.0	78	6.5	64	9.7	6
							10.1	5
							10.9	12
80 min	−17.5	51	8.1	100	6.5	82	1.8	14
							10.9	5
13 h			8.3	73	6.6	100	2.2	11
							9.9	3
43 h			8.3	46	6.7	100	2.3	1
							10.0	3
61 h			8.3	27	6.7	100	10.0	3
85 h			8.3	20	6.7	100	10.0	4
10 d			8.4	7	6.7	100	10.0	3

described previously; the complex scattering factors were those listed by Ross et al.[33]

Reaction of Diisopropyl(trimethylsilyl)phosphane 3 with Si_2Cl_6: Hexachlorodisilane (3.15 g, 11.7 mmol) was added dropwise to ice-cooled **1** (2.2 g, 11.6 mmol). A strongly exothermic reaction occurred. After 2 h stirring at room temperature, trimethylchlorosilane was distilled off from the red liquid; subsequent distillation at 2.5 mbar provided 2.3 g (78%) **4** as a colourless liquid, b.p. 65 °C.[34]

Reaction of *tert*-Butyl(isopropyl)(trimethylsilyl)phosphane 5[9] with Si_2Cl_6 Followed by Heteronuclear NMR: Hexachlorodisilane (0.43 g, 1.6 mmol) is added dropwise to ice-cooled **5** (0.33 g, 1.6 mmol). After warming up to room temperature, the brown liquid was transferred into an NMR tube. For results see Table 9.

NMR data of disilanylphosphane **7**: δ^{31}P 8.3 [s, $^1J(^{31}P, ^{29}Si) \pm 126.0$ Hz; $^2J(^{31}P, ^{29}Si) \pm 22.2$ Hz]; δ^{29}Si 13.2 [d, d, $^1J(^{31}P, ^{29}Si) \pm 125.5$ Hz; $^3J(^{29}Si, ^1H) \pm 8.7$ Hz], −0.4 [d, $^2J(^{31}P, ^{29}Si) \pm 24.0$ Hz].

Reaction of Di-*tert*-butyl(trimethylsilyl)phosphane (1) with the Disilane Fraction: A mixture of 6.21 g (28.43 mmol) of silylphosphane **1** and 12.52 g of a freshly distilled *WACKER AG.* technical disilane fraction sample [$Me_2(Cl)SiSiCl_2Me/(MeCl_2Si)_2$ ratio about 1:1; corresponding to about 28 mmol of each of the two disilanes] was heated to 100 °C. After 16 h, a ^{31}P-NMR spectrum confirms complete consumption of silylphosphane **1**. Distillation at 1 mbar allowed separation of two fractions: b.p. 55−60 °C, 1.6 g (24%) *t*Bu$_2$PSiMe$_2$Cl (**8**),[10] and b.p. 110−114 °C, 4.4 g (48%) *t*Bu$_2$PSi(Me(Cl)Si(Me)Cl$_2$ (**9**).

8: ^{1}H NMR: $\delta = 1.28$ (d, $J = \pm 11.4$ Hz, 18 H), 0.6 (d, $J = \pm 3.5$ Hz); ^{31}P NMR: $\delta = 0.8$ (s, ^1J (^{31}P, ^{29}Si = ± 67.5 Hz).[10]

NMR data of **9**: ^{1}H NMR: $\delta = 1.26$ [d, $^3J(^{31}P, ^1H) \pm 12$ Hz, PCCH_3, 18 H], 0.87 [d, $^3J(^{31}P, ^1H) \pm 3.7$ H, PSiCH_3,, 3 H], 0.78 (s, SiSiCH_3, 3 H). – ^{13}C NMR: $\delta = 34.2$ [d, $^1J(^{31}P, ^{13}C) \pm 26.5$ Hz, P*C*], 33.1 [d, $^2J(^{31}P, ^{13}C) \pm 12.4$ Hz, C-*C*H$_3$], 7.1 (s, SiSi-*C*), 4.9 [d, $^2J(^{31}P, ^{13}C) \pm 8.3$ Hz, PSi-*C*]. – ^{29}Si NMR: $\delta = 12.1$ [d, $^1J(^{31}P, ^{29}Si) \pm 100.2$ Hz, P-*Si*], 26.8 [d, $^2J(^{31}P, ^{29}Si) \pm 21.9$ Hz, PSi-*Si*]. – ^{31}P NMR: $\delta = 8.6$ [s, ^1J (^{31}P, ^{29}Si) ± 100.8 Hz, ^2J (^{31}P, ^{29}Si) ± 22.0 Hz].

Synthesis of Di-*tert*-butyl(pentamethyldisilanyl)phosphane (10): Methyllithium dissolved in ether (28.5 mL of a 1.6 M solution, 45.6 mmol) was added slowly to a solution of 4.52 g (13.8 mmol) **19** in ether at −20 °C. Stirring was continued for 2 h at room tempature, and subsequently the mixture was heated under reflux for 30 min. After separation of the solution from lithium chloride, dis-

Table 10. ^{31}P-NMR data of *t*Bu(*i*Pr)PGeMe$_3$ (**14**) and *t*Bu(*i*Pr)PSiCl$_3$ (**6**)

time	**14** [ppm]	relative intensity	**6** [ppm]	relative intensity	other signals [ppm]	relative intensity
5 min	−1.5	100	6.0	10	1.4	7
					3.0	7
					7.5 (*)	12
					11.8	4
3 h	−1.6	100	6.1	53	1.4	13
					3.1	14
					7.5 (*)	9
					11.7	4
15 h	−1.6	23	6.2	100	1.4	12
					3.5	22
					11.4	3
					11.9	3
6 d			6.5	100	1.5	8
					3.9	6

(*) Probably *t*Bu(*i*Pr)PSiCl$_2$SiCl$_3$ (**7**).

Table 11. ^{29}Si-NMR: of $Me_3GeSiCl_3$ **15**, $(Me_3Ge)_2Si(SiCl_3)_2$ **16**, $SiCl_4$

time	**15** [ppm]	relative intensity	**16** [ppm]	relative intensity	$SiCl_4$ [ppm]	relative intensity	other signals [ppm]	relative intensity
3 h	17.5	11	16.9	11	−19.0	100	10.1	43 (*)
15 h	17.7	19	16.8−84.9	307	−19.0	100	**3** (d,d): 10.1 (+), 10.4, 13.1, 13.3	38 (+), 27, 23, 25
7 d	17.9 (broad)	89	16.9	76	−19.0	89	**3**: 11.8 (d,d) **3**: 11.8	100 (++)
26 d	17.8 (broad)	71	16.9	74	−19.0	64	(d,d)	100 (++)

(*) Reasonable assignment: $Me_3GeSi(SiCl_3)_3$; (+) intensity of this peak of the d,d pattern enhanced due to overlap with the singlet at δ = 10.1 of (*); (++) normal intensity d,d pattern.

Table 12. ^{31}P-NMR data of *t*Bu(*i*Pr)$PSiCl_3$ (**6**), and *t*Bu(*i*Pr)PSi_2Cl_5 (**7**)

time	**7** [ppm]	relative intensity	**6** [ppm]	relative intensity	other signals [ppm]	relative intensity
20 min	8.1	6	6.3	100	1.2[a] 4.1	35
15 h			6.2	100	1.1[a]	2

[a] *t*Bu(*i*Pr)PH.

Table 13. ^{29}Si-NMR data of $(Me_3Sn)_2Si(SiCl_3)_2$ (**19a**), and *t*Bu(*i*Pr)$PSiCl_3$ (**3**)

time	**19a** [ppm]	relative intensity	$SiCl_4$ [ppm]	relative intensity	other signals [ppm]	relative intensity
60 min	19.4	58	−19.2	100	11.2 (*) **3:** 11.8 (d,d)	36 38, 38, 36, 25
15 h	19.4 −106.6	64 11	−19.2	100	**3**: 11.8 (d,d) 11.3 (*), −88 (*)	35, 35, 33, 33 21, 3

(*) $Me_3SnSi(SiCl_3)_3$ (**20a**).

tillation yielded 2.5 g (66%) of disilanylphosphane **10** as a colourless liquid. − ^{1}H NMR: δ = 1.29 [d, ^3J (^{31}P, ^{1}H) ± 11.1 Hz, PCC*H*$_3$, 18 H], 0.38 [d, ^3J(^{31}P, ^{1}H) ± 4.1 Hz, PSiC*H*$_3$, 6 H], 0.18 [s, SiSiC*H*$_3$), 9H]. ^{13}C NMR: δ = 33.5 [d, ^2J(^{31}P, ^{13}C) ± 12.1 Hz, C*C*H$_3$], 32.8 [d, ^1J(^{31}P, ^{13}C) ± 24.9 Hz, P*C*], 4.9 [d, ^2J(^{31}P, ^{13}C) ± 11 Hz, PSi-*C*]. −0.6 [d, ^3J(^{31}P, ^{13}C) ± 1.2 Hz, SiSi-*C*]. − ^{29}Si NMR: δ = −25.2 [d, ^1J(^{31}P, ^{29}Si) ± 63.4 Hz, P-*Si*], −14.9 [d, ^2J(^{31}P, ^{29}Si) ± 12.1 Hz, PSi-*Si*]. − ^{31}P NMR: δ = 5.6 [s, ^1J (^{31}P, ^{29}Si) ± 63.6 Hz, ^2J (^{31}P, ^{29}Si) ± 12.5 Hz]. − MS (EI, 70 eV) *m*/*z*(%): 276 (3, M^+), 131 (22, $Me_5Si_2^+$), 73 (60, Me_3Si^+), 58 (100, $C_4H_{10}^+$). − IR (liquid between KBr) [cm^{-1}] 2970 (s), 2950 (vs), 2900 (s), 2870 (s) 1475 (m), 1395 (m), 1370 (m), 1250 (s), 1200 (w), 1165 (m), 1045 (m), 1005 (m), 945 (m), 920 (m), 895 (w), 835 (s), 810 (s), 780 (m), 740 (vw), 690 (vw), 675 (w), 620 (w), 540 (vw), 495 (w), 440 (vw). − $C_{13}H_{33}PSi_2$ (276.55), found (calc.) C 56.19 (56.46), H 11.83 (12.02), P 11.13 (11.20).

Reaction of Diisopropyl(trimethylsilyl)amine (11) with Si_2Cl_6: Hexachlorodisilane (7.35 g, 27.3 mmol) was added to 4.5 g (26 mmol) diisopropyl(trimethylsilyl)amine. After heating the mixture for 6 h at 60°C complete consumption of the silylamine was indicated by NMR. Distillation at 0.5 mbar gave 6.24 g (72%) diisopropyl(pentachlorodisilanyl)amine as a moisture-sensitive colourless liquid, b.p. 61°C.[35] − ^{1}H NMR: δ = 1.02 [d, ^3J($^{1\,H,\,1}$H) ± 6.7 Hz, C*H*$_3$,, 12 H], 3.26 [sept, ^3J($^{1\,H,\,1}$H) ± 6.7 Hz, C*H*, 2 H]. − ^{13}C NMR: δ = 23.55 (s, *C*H$_3$), 47.25 (s, *C*H). ^{29}Si NMR: δ = −1.8 (s), −26 (s). − MS (EI, 70 eV): *m*/*z* (%) 318 (14) [M^+ − CH_3]; 276 (14) [M^+ − CH_3, − C_3H_6]; 176 (12) [M^+ − CH_3, − C_3H_6, − $SiCl_2$]; 133 (18) [$SiCl_3^+$]; 98 (4) [$SiCl_2^+$], 44 (100) [$C_3H_8^+$]. − IR $\tilde{\nu}$ (liquid between KBr) [cm^{-1}]: 2970 (s), 2939 (s), 2880 (s), 2850 (m) 1460 (m), 1385 (m), 1370 (s), 1305 (w), 1205 (w), 1175 (m), 1155 (w), 1000 (w), 885 (m), 840 (m), 815 (w), 800 (w), 645 (m), 570 (vs, broad), 510 (s), 485 (m), 445 (s), 375 (m). − $C_6H_{14}Cl_5NSi_2$ (336.62) found (calcd.) C 21.56 (21.41), H 4.14 (4.19), Cl 53.03 (52.66).

Reaction of Diisopropyl(trimethylstannyl)amine 12 with Si_2Cl_6: Hexachlorodisilane (2.7 g, 10 mmol) was added slowly at 0°C to 2.45 g (9.3 mmol) diisopropyl(trimethylstannyl)amine. After warming up to room temperature, complete consumption of the stannylamine was indicated by NMR. After removal of Me_3SnCl by crystallisation from pentane, distillation at 0.8 mbar gave 1.3 g (40%) diisopropyl(pentachlorodisilanyl)amine (**13**) as a moisture-sensitive colourless liquid,[35] b.p. 65°C (see above).

Table 14. ^{119}Sn-NMR data of $Me_3SnSiCl_3$ (**18a**) and $(Me_3Sn)_2Si(SiCl_3)_2$ (**19a**)

time	**18a** [ppm]	relative intensity	**19a** [ppm]	relative intensity
15 min	−66.3	26	−53.5	100
15 h	−66.5	4	−53.5	100

Table 15. ^{31}P-NMR data of *t*Bu(*i*Pr)$PSiCl_3$ (**6**), and *t*Bu(*i*Pr)PSi_2Cl_5 (**7**)

time	**7**		**6**		other signals	
	[ppm]	relative intensity	[ppm]	relative intensity	[ppm]	relative intensity
5 min	8.5	100	6.7	19	1.1	27
					4.3	2
30 min	8.4	63	6.6	100	1.2	26
					4.3	2
70 min	8.4	16	6.6	100	1.2	8
					4.2	1
5 h			6.5	100	1.1	6
3 d			6.6	100	1.2	1

Table 16. ^{119}Sn-NMR data of $Et_3SnSiCl_3$ (**18b**), $(Et_3Sn)_2Si(SiCl_3)_2$ (**19b**), and Et_3SnCl

time	**18b** [ppm]	relative intensity	**19b** [ppm]	relative intensity	Et_3SnCl [ppm]	relative intensity
25 min	−58.4	100	−44.6	17	150 (*)	6
60 min	−58.5	87	−44.7	100	145 (*)	7
330 min	−58.7	12	−44.8	100	136 (*)	7
24 h	−58.6	9	−44.8	100	135 (*)	7
3 d	−58.6	7	−44.8	100	135 (*)	8
9 d	−58.5	8	−44.8	100	135 (*)	8

(*) Broad.

Reaction of *tert*-Butyl(isopropyl)(trimethylgermyl)phosphane 14 with Si_2Cl_6 Followed by Heteronuclear NMR: Hexachlorodisilane (0.35 g, 1.3 mmol) was added dropwise to ice-cooled **14** (0.33 g, 1.3 mmol). A violet precipitate could be observed. After warming up to room temperature, the brown liquid was transferred into an NMR tube. For NMR results see Tables 10 and 11.

Reaction of *tert*-butyl(isopropyl)(trimethylstannyl)phosphane 17a with Si_2Cl_6 followed by heteronuclear NMR: Hexachlorodisilane (0.4 g, 1.5 mmol) was added dropwise to ice-cooled **17a** (0.41 g, 1.4 mmol). A red precipitate could be observed. After warming up to room temperature, the yellow liquid was transferred into an NMR tube. For NMR results see Tables 12, 13, and 14.

Reaction of *tert*-Butyl(isopropyl)(triethylstannyl)phosphane (17b) with Si_2Cl_6 Followed by Heteronuclear NMR: Hexachlorodisilane (0.24 g, 0.89 mmol) was added dropwise to ice-cooled **17b** (0.29 g, 0.86 mmol). The liquid turned red, then yellow and, at room temperature, green. The green liquid was transferred into an NMR tube. For NMR results see Table 15.

^{29}Si-NMR after 5 h: [$SiCl_4$: relative intensity = 100%] δ^{29}Si = 21.0/−108.1 (50%/9%) [$(Et_3Sn)_2Si(SiCl_3)_2$ (**19b**)], 11.8 (d,d) (4 lines, 20% each) [*t*Bu(*i*Pr)$PSiCl_3$ (**6**)], 12.1 (35%)[20b]; in a separate experiment, a spectrum with about 12 h acquisition time allowed the resolution of two signals for **20b**: δ^{29}Si = 11.7 ($SiCl_3$), −88.0 [$Si(SiCl_3)_3$]. For NMR results see Table 16.

Reaction of *tert*-Butyl(isopropyl)(tri-*n*-butylstannyl)phosphane (17c) with Si_2Cl_6 Followed by Heteronuclear NMR: Hexachlorodisilane (0.27 g, 1.0 mmol) was added dropwise to ice-cooled **17c** (0.4 g, 0.95 mmol). After warming up to room temperature, the greenish-yellow solution was transferred into an NMR tube (see the following tables).

Adding excess of the disilane (0.4 g, 1.5 mmol) at −20 °C to **17c** (0.27 g, 1.0 mmol) led qualitatively to the same products, but in a quite different distribution (faster consumption of **7** and of **18c**;

Table 17. ^{31}P-NMR data of *t*Bu(*i*Pr)$PSiCl_3$ (**6**) and *t*Bu(*i*Pr)$PSiCl_2SiCl_3$ (**7**)

time	**7**		**6**		other signals	
	[ppm]	relative intensity	[ppm]	relative intensity	[ppm]	relative intensity
2 h	7.3	100	5.9	9	1.4	3
					10.3	3
2.5 h	7.3	100	5.9	21	1.4	3
					10.3	.
12 d	7.0	3	5.9	100		

Table 18. ^{119}Sn-NMR data of *n*$Bu_3SnSiCl_3$ (**18c**), $(nBu_3Sn)_2Si(SiCl_3)_2$ (**19c**) and *n*$Bu_3SnSi(SiCl_3)_3$ (**20c**)

time	**18c** [ppm]	relative intensity	**20c** [ppm]	relative intensity	other signals [ppm]	relative intensity
2.5 h	−72.3	100			45.5	57
12 d	−72.7	21	−48.1	100		
75 d			−47.8	100	−53.8 (*)	64
					142.0 (**)	59

(*) **19c**; (**) *n*Bu_3SnCl.

about 5:4 intensity ratio of the ^{119}Sn-NMR signals of **19c** and **20c** after 30 days). For NMR results see Tables 17 and 18.

Acknowledgments

We thank the Deutsche Forschungsgemeinschaft, Bonn-Bad Godesberg, and the Fonds der Chemischen Industrie, Frankfurt, for financial support, the WACKER AG, Burghausen, for a sample of the disilane fraction, and Professor Uwe Klingebiel (Universität Göttingen) for a ^{29}Si-NMR measurement. We thank the U. K. Engineering and Physical Sciences Research Council for a research studentship (P. M. P.), for support of the Edinburgh gas electron diffraction Service (grant GR/K 44411) and *ab initio* calculations (grant GR/K 04194) and for provision of microdensitometer facilities at the Daresbury Laboratory.

[1] R. Martens, W.-W. du Mont, *Chem. Ber.* **1993**, *126*, 1115−1117.
[2] L.-P. Müller, W.-W. du Mont, J. Jeske, P. G. Jones, *Chem. Ber.* **1995**, *128*, 615; L.-P. Müller, A. Zanin, W.-W. du Mont, J. Jeske, P. G. Jones, *Chem. Ber.* **1997**, *130*, 377.
[3] R. A. Benkeser, *Acc. Chem. Res.* **1971**, *4*, 94.
[4] R. A. Benkeser, K. M. Foley, J. B. Grutzner, W. E. Smith, *J. Am. Chem. Soc.* **1970**, *92*, 697.
[5] W.-W. du Mont, L.-P. Müller, L. Müller, S. Vollbrecht, A. Zanin, *J. Organomet. Chem.* **1996**, *521*, 417.
[6] W.-W. du Mont, L.-P. Müller, L. Müller, S. Vollbrecht, A. Zanin, XI. Int. Symp. on Organosilicon Chemistry, Montpellier **1996**, Abstract.
[7] L. Müller, W.-W. du Mont, F. Ruthe, P. G. Jones, H. C. Marsmann, *J. Organomet. Chem.*, in print
[8] R. Martens, W.-W. du Mont, *Chem. Ber.* **1992**, *125*, 657.
[9] L. Müller, W.-W. du Mont, F. Ruthe, P. G. Jones, to be published; L. Müller, Ph.D. thesis, TU Braunschweig, **1998**.
[10] H. Schumann, W.-W. du Mont, *Z. Anorg. Allg. Chem*. **1975**, *418*, 259.
[11] G. D. Cooper, A. R. Gilbert, *J. Am. Chem. Soc.* **1960**, *82*, 5042.
[12] G. Urry, *Acc. Chem. Res.* **1970**, *3*, 306.
[13] U. Herzog, R. Richter, E. Brendler, G. Roewer, *J. Organomet. Chem.* **1996**, *507*, 221.
[14] H. J. Emeleus, M. Tufail, *J. Inorg. Nucl. Chem.* **1967**, *29*, 2081.
[15] U. Herzog, G. Roewer, U. Pätzold, *J. Organomet. Chem.* **1996**, *494*, 143.
[16] U. Herzog, G. Roewer, *J. Organomet. Chem.* **1997**, *544*, 217.
[17] K. G. Sharp, P. A. Sutor, E. A. Williams, J. D. Cargioli, T. C. Farrar, K. Ishibitsu, *J. Amer. Chem. Soc.* **1976**, *98*, 1977.
[18] G. Fritz, H. Schäfer, *Z. Anorg. Allg. Chem.* **1974**, *407*, 295.
[19] ASYM 40, version 3.0, update to program ASYM 20: L. Hedberg, I. M. Mills, *J. Mol. Spectrosc.* **1993**, *160*, 117.
[20] A. J. Blake, P. T. Brain, H. McNab, J. Miller, C. A. Morrison, S. Parsons, D. W. H. Rankin, H. E. Robertson, B. A. Smart, *J. Phys. Chem.*, **1996**, *100*, 12280; P. T. Brain, C. A. Morrison, S. Parsons, D. W. H. Rankin, *J. Chem. Soc.*, *Dalton Trans.*, **1996**, 4589.
[21] C. Glidewell, P.M. Pinder, A.G. Robiette, G.M. Sheldrick, *J. Chem. Soc.*, *Dalton Trans.*, **1972**, 1402.
[22] R. Demuth, H. Oberhammer, *Z. Naturforsch. A*, **1973**, *28*, 1862.
[23] *Gaussian 94* (Revision C.2), M. J. Frisch, G. W. Trucks, H. B. Schlegel, P. M. W. Gill, B. G. Johnson, M. A. Robb, J. R. Cheesman, T. A. Keith, G. A. Petersson, J. A. Montgomery, K. Raghavachari, M. A. Al-Laham, V. G. Zakrzewski, J. V. Ortiz, J. B. Foresman, J. Cioslowski, B. B. Stefanov, A. Nanayakkara, M. Challacombe, C. Y. Peng, P. Y. Ayala, W. Chen, M. W. Wong, J. L. Andres, E. S. Replogle, R. Gomperts, R. L. Martin, D. J. Fox, J. S. Binkley, D. J. Defrees, J. Baker, J. P. Stewart, M. Head-Gordon, C. Gonzalez, J. A. Pople, Gaussian Inc., Pittsburgh, PA, **1995**.
[24] J. S. Binkley, J. A. Pople, W. J. Hehre, *J. Am. Chem Soc.*, **1980**, *102*, 939.
[25] M. S. Gordon, J. S. Binkley, J. A. Pople, W. J. Pietro, W. J. Hehre, *J. Am. Chem. Soc*., **1982**, *104*, 2797.
[26] W. J. Pietro, M. M. Francl, W. J. Hehre, D. J. Defrees, J. A. Pople, J. S. Binkley, *J. Am. Chem. Soc.*, **1982, 104**, 5039.
[27] W. J. Hehre, R. Ditchfield, J. A. Pople, *J. Chem. Phys.*, **1972, 56**, 2257.
[28] P. C. Hariharan, J. A. Pople, *Theor. Chim. Acta*, **1973**, *28*, 213.
[29] M. S. Gordon, *Chem. Phys. Lett*. **1980**, *76*, 163.
[30] C. M. Huntley, G. S. Laurenson, D. W. H. Rankin, *J. Chem. Soc.*, *Dalton Trans.* **1980,** 954.
[31] S. Cradock, J. Koprowski, D. W. H. Rankin, *J. Mol. Struct.* **1981**, *77*, 113.
[32] A. S. F. Boyd, G. S. Laurenson, D. W. H. Rankin, *J. Mol. Struct.* **1981**, *71*, 217.
[33] A. W. Ross, M. Fink, R. Hildebrandt, in: *International Tables for Crystallography*, Vol. C, (Ed.: A. J. C. Wilson), Kluwer Academic Publishers, Dordrecht, **1992**, p. 245.
[34] R. Martens, W.-W. du Mont, L. Lange, *Z. Naturforsch. B* **1991**, *46*, 1609.
[35] H. Schuh, T. Schlosser, P. Bissinger, H. Schmidbaur, *Z. Anorg. Allg. Chem.* **1993**, *619,* 1347.

Received December 28, 1998
[I98451]